10.1109/ULTSYM.2012.0059

Real-time, transcranial monitoring of safe blood-brain barrier opening in non-human primates

Fabrice Marquet[1], Shih-Ying Wu[1], Yao-Sheng Tung[1], Tobias Teichert[2], Matthew Downs[1,2], Shutao Wang[1],Vincent P. Ferrera[2] and Elisa E. Konofagou[1,3]

Departments of [1]Biomedical Engineering, [2]Neuroscience and [3]Radiology, Columbia University, New York, NY, USA

fm2364@columbia.edu

Abstract — **The delivery of drugs to specific neural targets faces two fundamental problems: most drugs do not cross the blood-brain barrier and those that do spread to all parts of the brain. To date there exists only one non-invasive methodology with the potential to solve these problems: selective blood-brain barrier disruption using micro-bubble enhanced focused ultrasound. We have recently developed a single-element 500 kHz spherical transducer ultrasound setup for use in the non-human primate. Here, we tested the accuracy of the system by targeting the caudate nucleus of the basal ganglia in two macaque monkeys. Our results show that average in-plane error of the system is on the order of 2 mm and targeting error in depth, i.e., along the ultrasound path, is even smaller averaging 1.2 mm. We have also developed a real-time treatment monitoring based on backscattered emissions spectral analyses. This technique helped us determining a safe and reliable acoustic parameters window for BBB opening.**

Keywords- Focused ultrasound, blood-brain barrier, transcranial focusing.

I. Introduction

The main limiting factor towards the development of novel treatments of neurological and neurodegenerative diseases is the blood-brain barrier (BBB): more than 98% of small-molecule drugs and nearly all large-molecule drugs do not cross this anatomic barrier [1,2]. The blood-brain barrier (BBB) is a selective barrier within the neurovascular unit formed by the endothelial cells that line cerebral microvessels [3,4]. The BBB hinders the effective systemic delivery of neurological agents and biomarkers to the brain through a combination of passive, transport and metabolic barriers. Very small gaseous molecules and small molecules presenting high lipid solubility can diffuse freely through the lipid membranes. The main role of the BBB is to control the flow of nutrients from the lumen to the parenchyma and therefore to maintain the brain homeostasis for proper neuronal firing [5]. Several techniques exist to circumvent the BBB, such as intracranial injections, mixing or attaching agents to BBB-modifying chemicals, and the chemical alteration of agents to be delivered through endogenous transport systems [2,6]. However, these techniques are either invasive, drug-specific or are plagued by very poor spatial specificity. Microbubble-enhanced, focused ultrasound (ME-FUS) has been proven to be capable of disrupting the BBB noninvasively, transiently and selectively in small animals [7,8,9] usually using frequencies above 1 MHz. Initial proof of concept in non-human primates has also been shown [10]. There are three critical requirements for this technique before undergoing clinical applications. ME-FUS needs to be proven safe. This encompasses determining a reliable set of acoustic parameters, monitoring the treatment real-time and understanding the BBB closing timeline. ME-FUS also needs to be proven accurate in order to deliver therapeutic agents only in the desired region of the brain. Finally, the treatment time must be optimized as it is currently the most important shortcoming for therapeutic ultrasound.

II. Methods

A. ME-FUS

A 500-kHz center frequency focused ultrasound transducer was used for this experiment (Sonic Concepts, WA, USA). A flat-band spherical hydrophone was mounted in the bore hole of the therapeutic transducer. The acoustic parameters used for the three protocols were the following: focal maximum estimated pressure of 0.2 MPa to 0.3 MPa, pulse length of 10 ms, pulse repetition frequency of 2 Hz, total sonication duration of 2 min. An inflatable urethane membrane was mounted on top of the transducer. The rate of inflation was controlled by a degassing system composed by a circulation pump and a vacuum pump to prevent dissolved oxygen to induce unwanted cavitation. The transducer-hydrophone assembly was attached to a Kopf stereotaxic manipulator to enable targeting of the ultrasound focus in stereotactic coordinates for accurate positioning (Fig. 1). This setup optimizes the procedure time as the animals stayed in the stereotactic frame less than 20 minutes per treatment.

In vitro pressure measurements were realized in another study [11]. This study determined the global attenuation (absorption, reflexion and scattering) due to the presence of

This study was supported in part by the National Institutes of Health (R01EB009041, R01MH059244, R01AG038961) and NSF CAREER 0644713. DFG 819/1-1. Kavli Institute.

the skull (around -5.7 dB at 500 kHz). The attenuation in the skin was assumed to be around −0.9 dB.cm−1 and its thickness was estimated to be equal to 0.5 cm. The attenuation in the monkey brain tissue was assumed to be around −0.5 dB.cm−1 and the thickness of this layer was estimated to be equal to 2 cm. Therefore, the emission amplitude has to be raised by 7.15 dB (approximately a factor 2.28) compared to the calibration measurements in water to compensate for the energy loss along the path. Before sonication, IV injection of custom made monodispersed lipid-shelled microbubbles (4-5µm mean diameter) was performed. All monkey experiments were carried out in accordance with the Columbia University Institutional Animal Care and Use Committee.

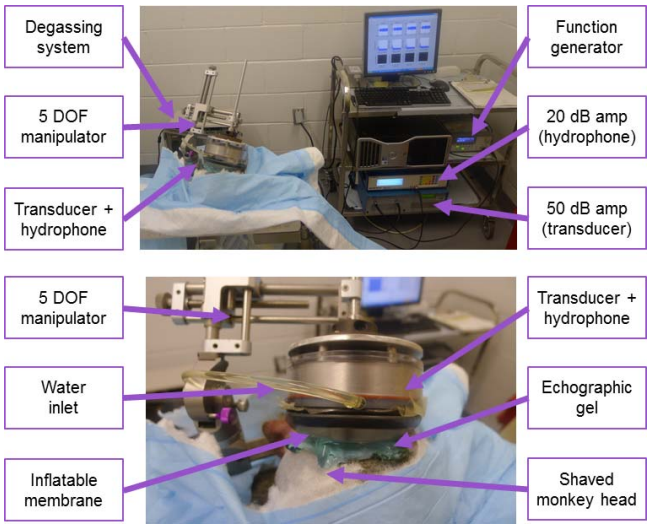

Fig 1. Preclinical setup. Top picture is showing a large view of the operating room. On the right, the PC and amplifiers are used to drive the transducer-hydrophone assembly. The degassing system (vacuum pump + water circulation pump) ensures a constant flow of degassed water for acoustic coupling. The transducer-hydrophone assembly is mounted on a manipulator with 5 degrees of freedom. Bottom picture is depicting a close-up view. The membrane can be inflated regulating the water flow thanks to the degassing system. This ensures a maximal acoustic transmission in the animal brain.

B. *Real-time monitoring*

Backscattered acoustic emissions were recorded. Online spectrum analyses were performed to study the bubble activity at the focus. In order to remove the harmonic (nf, n = 1, 2, …,6), sub-harmonic (f/2) and ultra-harmonic (nf/2, n = 3, 5, 7, 9) frequencies produced by stable cavitation [12], the response within a 300-kHz bandwidth around each harmonic and 100-kHz bandwidth of each sub- and ultra-harmonic frequency were excluded to get only the broadband signal. From those sets of two spectra, both the broadband and total energies are computed by summing the spectral amplitudes. Two metrics are then defined as indications of inertial and stable cavitation by analyzing the differences between backscattered with and without bubbles.

The broadband energy increase (BEI) was monitored as an indication of inertial cavitation and was defined as follow:

$$BEI = 10\log\left(\frac{\mathcal{E}_{bubble}^{broadband}}{\mathcal{E}_{control}^{broadband}}\right)$$

The harmonic energy is obtained by subtracting the broadband energy to the total energy. The harmonic energy increase is an indication of stable cavitation and was defined as follow:

$$HEI = 10\log\left(\frac{\mathcal{E}_{bubble}^{total} - \mathcal{E}_{bubble}^{broadband}}{\mathcal{E}_{control}^{total} - \mathcal{E}_{control}^{broadband}}\right)$$

C. *MRI*

After sonication, the anesthetized animals were transported to the MR facility where T2 and T2 FLAIR images were taken to detect any potential damage caused by the sonication. The integrity of the BBB was tested using the T1 contrast agent gadodiamide (Omniscan) that is typically used to visualize the break-down of the BBB in neurological disease. To that aim, a high-resolution structural T1 image was recorded prior to the injection of gadodimide (T1 Pre; 3D Spoiled Gradient-Echo, TR/TE = 20/1.4 ms; flip angle: 30°; NEX = 2; in-plane resolution: 1x1 mm2; slice thickness: 1 mm with no interslice gap). 30 min after injection of 0.15 ml/kg gadodiamide IV, another T1 image was acquired using identical scanning parameters (T1 Post). As gadodiamide does not cross the intact BBB, increased T1 signal strength will indicate regions with increased BBB permeability.

To estimate gadodiamide concentration [Gd]c we divided the post T1 image by the pre T1 image (post/pre). The post/pre image highlights regions of increased T1 contrast following the injection of gadodiamide. This includes regions of interest where the BBB was disrupted, but also any vessels or other regions with high blood volume such as the pial surface. The post/pre image was then flipped such that the left hemisphere overlaid the right hemisphere. The un-flipped image was then divided by the flipped image. This procedure removed activations due to high [Gd] in voxels with high blood-volume, as long as the regions were symmetric between the hemispheres. The resulting image that formed the basis of our analysis highlights increased [Gd] in the sonicated region, as well as some residual artificial activation mainly due to asymmetric vasculature.

To assess the targeting accuracy, the resulting image was rotated and shifted into a new coordinate frame where the origin was defined as the predicted location of the ultrasound focus, and the z-axis corresponded to the approach angle (Figure 3). We selected a region of interest around the origin corresponding to ±7.5 mm in the lateral plane, and -5 to +12 mm along the axial dimension. A voxel was defined as being

"opened" when the T1-enhancement exceeded a threshold of 10%. The total volume of the BBB opening was quantified as the volume of the opened voxels in the region of interest round the sonication target. The fraction of opened voxels was then averaged across the z-axis. Based on this two-dimensional x-y map, the core-region of the opening was defined as pixels with more than an average of 35% of opened voxels.

III. Results

Firstly, real-time monitoring was thoroughly tested to calibrate BEI and HEI at different pressure. These results can be seen in Fig 2. Based on previous results [10], the lowest pressure at which BBB opening was achieved is 0.2 MPa while the damage detection threshold was 0.45 MPa. One can see a strong correlation between the BBB opening threshold and the HEI whereas the BEI might be a good parameter to monitor to detect damages. This is why in this study the pressure range was set to 0.2 MPa – 0.3 MPa.

Examples of five different sonications targeting the caudate are displayed on Fig 3. These results prove the reproducibility and targeting precision of the FUS technique. In Fig. 3, the top row shows the fraction of activated voxels in the lateral plane. Averaged over all sonications in both animals, the average absolute lateral error was 1.1 mm with a standard deviation of 0.8 mm. The second row shows the fraction of activated voxels as a function of the depth. On average, the focus was 4.1±0.2 mm dorsal to the intended focal point. This finding closely matches the ~5 mm shift of the focal depth that was predicted by an *in vitro* study with immersed skull [11]. After correcting for the predicted focal shift, the average absolute targeting error along the depth-axis was 0.3±0.2 mm. At this pressure range only one sonication with 0.2 MPa failed to elicit any detectable opening (data not shown).

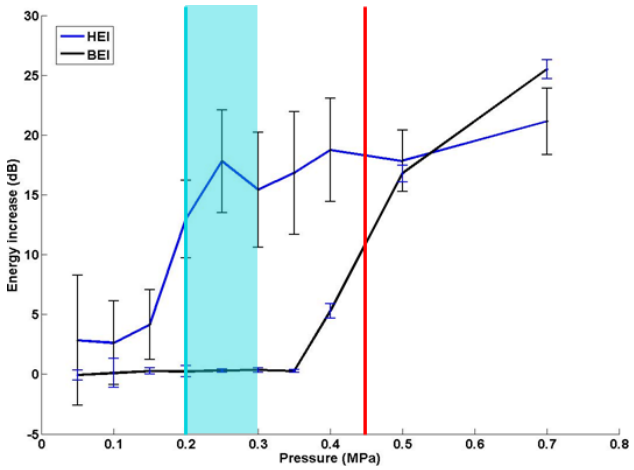

Fig.2. Harmonic and broadband energy increase calibration along different pressure levels. The light blue line corresponds to the lowest pressure at which BBB opening was achieved, the red line corresponds to the damage detection threshold using MRI. The light blue area is the pressure range chosen for this study.

The real-time monitoring of the backscattered signal was proven to be a very good way to characterize the bubble activity. All experiments showed significant HEI (at least 15 dB) when the bubbles are flowing into the animal system. This indicates that the bubbles, excited by the transducer, are exerting stress on the vessel walls. On the other hand no BEI was recorded. A 3dB threshold, corresponding approximately to 3 standard deviations of the negative controls, had been set and was never crossed.

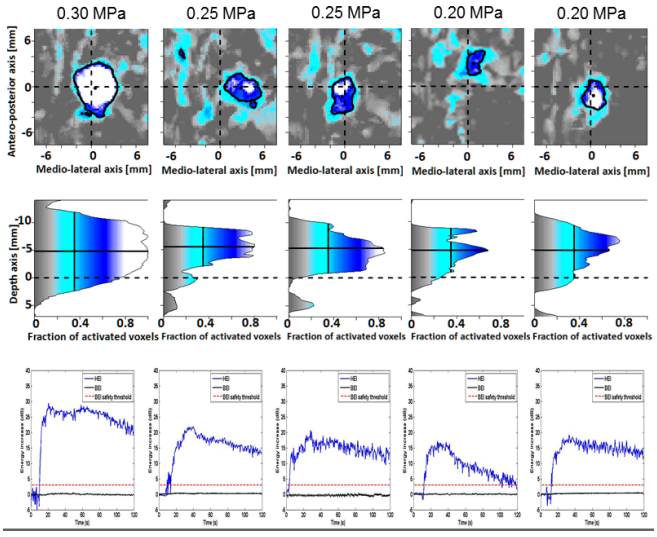

Fig 3. Results for 5 different sonications. Top row depicts distribution of the fraction of activated voxels in the lateral plane. The black contour delineates the region where the BBB is opened. Middle row shows the fraction of activated voxels as a function of the depth. The 5-mm shift towards the transducer was predicted by *in vitro* experiments and is therefore correctible. The last row displays the corresponding HEI / BEI real-time monitoring. The harmonic signal exhibited each time a significant increase whereas the broadband increase remained neglectable.

IV. Conclusion

The reported experiments demonstrate that a single spherical transducer operating at an intermediate frequency of 500 kHz can be used for accurate, repeatable and localized blood-brain barrier disruption in deep subcortical structures. This constitutes an important step towards developing a non-invasive targeted drug-delivery system. This method showed tremendous potential for clinical treatments of neurodegenerative diseases and also for neuroscientists, who want dissect the function of deep-seated regions of the brain such as the basal ganglia. Real-time monitoring was found to be a great mean of understanding how the bubbles react while activated by the transducer. Two reliable metrics for BBB opening determination and potential damage threshold were defined and tested. Before clinical translation, a full study of the closing timeline must be performed.

Acknowledgment

The authors appreciate Girma Asfaw, Department of Neuroscience, Columbia University, for providing surgical assistance, Cherry Chen, Ph.D., Department of Biomedical Engineering, Columbia University for the manufacture of

the microbubbles and Stephen M. Dashnaw, Department of Biomedical Engineering, Columbia University, for his help in MRI scanning.

REFERENCES

1. A. Dove, *Nat. Biotechnol.*, **26**, 1212-1215 (2008).
2. W. M. Pardridge, *NeuroRX*, **2**, 3-14 (2005).
3. W. Risau and H. Wolburg, *Trends Neurosci.*, **13**, 174-178 (1990).
4. N. J. Abbott and I. A. Romero, *Mol. Med. Today*, **2**, 106-113 (106-113).
5. N. J. Abbott, L. Ronnback and E. Hansson, *Nat. Rev. Neurosci.*, **7**, 41-53.
6. W. M. Pardridge, *Drug Discov. Today*, **12**, 54-61 (2007).
7. G. Mychaskiw, A. E. Badr, R. Tibbs, B. R. Clower and J. H. Zhang, *Anesth. Analg.*, **91**, 798-803 (2000).
8. K. Hynynen, N. McDannold, N. Vykhodtseva, F. A. Jolesz, *Radiology*, **220**, 640-646.
9. J. J. Choi, M. Pernot, S. A. Small, E. E. Konofagou, *Ultra. Med. Biol.* **33**, 95-104.
10. F. Marquet, Y. S. Tung, T. Teichert, V. Ferrera, E. E. Konofagou, *PLoS ONE* **6(7)**, e22598 (2011).
11. F. Marquet, Y.S. Tung and E.E. Konofagou, *NanoLife* **1**, 309-322 (2010).